05,10

# Multiparticle complexes in encapsulated monolayers of transition metal dichalcogenides

© V.E. Bisti[1], G.M. Golyshkov[1,2], A.S. Brichkin[1], A.V. Chernrnko[1]

[1] Osipyan Institute of Solid State Physics RAS,
Chernogolovka, Russia
[2] Center for Photonics and 2D Materials, Moscow Institute of Physics and Technology,
Dolgoprudnyi, Russia

E-mail: bisti@issp.ac.ru

*Received June 30, 2025*
*Revised July 22, 2025*
*Accepted July 25, 2025*

The formation of multiparticle complexes in structures consisting of monolayers of transition metal dichalcogenides encapsulated by hexagonal boron nitride was studied. The binding energies of trions and excitons localized on charged impurities were calculated for interactions considered as charge-dipole interactions at long distances and approximated in two different ways at short distances. The range of polarizability values was chosen so that the obtained binding energies of the complexes were close to those observed experimentally. Comparison of the calculations allowed us to estimate the permissible range of exciton polarizability and identify the most realistic approximation of the dipole-charge interaction at short distances. The electron concentration was estimated from the intensity ratio of excitons and multiparticle complexes in the reflectance spectrum.

**Keywords:** transition metal dichalcogenides, boron nitride, trions and excitons.

DOI: 10.61011/PSS.2025.09.62368.1-25

## 1. Introduction

Monolayers of transition metal dichalcogenides (TMD) are two-dimensional semiconductors with a band gap that corresponds to energy of interband transitions in the visible range, thereby making them suitable for being studied by optical methods. TMD-based heterostructures can be of various types: TMD layers on a $SiO_2$/Si substrate; TMD monolayers encapsulated by hexagonal hBN, on the substrate; heterostructures covered by graphene layers. Coulomb interaction in the TMD monolayers due to dielectric environment can be enhanced or attenuated as compared to bulk materials or suspended monolayers. Covering these structures with the graphene layers makes it possible to energize the heterostructures, measuring structure parameters at the same time. A binding energy of excitons can be up to several hundred of meV, thereby making it possible to observe exciton effects at the temperatures up to the room one [1–3]. The energies of excitons in the TMD layers are experimentally determined and there are well-designed methods of calculation, which agree with experimental values [4,5]. The TMD monolayers have equilibrium charge carriers — electrons or holes which arrive from impurity centers in the surrounding hBN layers [4,5]. Some of them are localized due to interaction with ionized centers, while others are free and form a Fermi gas. A concentration of the charges can also be changed by energizing directly the TMD layer [8].

Excitations in the structures are studied by means of spectra of reflection, absorption and luminescence. Main excitations in the systems in question are interband excitons. Interaction of exciton with the equilibrium electrons significantly affects the observed spectra. The spectra of luminescence distinctly exhibit two lines that are interpreted as lines of radiative recombination of an exciton and a trion [1]. The spectra of reflection exhibit lines of the ground and excited states of the exciton and at certain conditions also show low-energy lines that are associated with the trions. It should be noted that it is no doubt that a high-energy line is a line of luminescence of the exciton. It is a generally accepted point of view, which is confirmed theoretically and experimentally [1–3]. But for the line interpreted as the trion line, other explanations are possible. Thus, when studying luminescence of quantum wells in GaAs/AlGaAs [9,10], it was shown when investigating a temperature and a magnetic-field dependence that the lines that had been previously ascribed to the free trion should have been related to a bound state of a multi-particle complex, namely, the exciton bound at a neutral donor or acceptor in a barrier.

Depending on used experimental methods, different approaches to theoretical consideration of the interband excitations in the TMD layers are applied. There are two approaches to taking into account Coulomb interaction of excitons with electrons: formation of trions (the bound states of the exciton and the electron) [11,3] or Fermi polarons (due to interaction of the excitons with a Fermi sea of the electrons) [12–17]. At low concentrations of the free electrons $n_s$ both the considerations are equivalent [3,16]. Interpretation by means of formation of three-particle complexes is true provided that $E_F \ll E_T$, where $E_F$ — the energy of the Fermi gas of electrons, $E_T$ — the binding energy of the trion, but a respective peak in absorption or reflection is small as compared to the exciton peak. The trion peak is distinctly observed and comparable in intensity to the exciton peak only when $E_F \sim E_T$. It should be noted that in the structures with the TMD layers always $E_x \gg E_F$, $E_T$, where $E_x$ — the exciton binding energy.

The study [12] was the first to propose the influence of interaction of the interband excitons with excitations of the electron Fermi system of a particle-hole type (Suris tetrons).

The idea of the Fermi polarons was used when studying two-component ultra-cold gases. When an impurity atom is absorbed in the Fermi gas with a short-range attractive potential of interaction between the impurity atom and the gas particles, there are two lines that correspond to the „attracting" and „repelling" polarons [13–15].

A concept of the excitons surrounded by a cloud of the electron-hole pairs excited from the Fermi sea turned out to be fruitful for describing the spectra of reflection or absorption in the structures with the TMD layers not only at small, but intermediate values of $n_s(E_F \sim E_T)$ [16,17] as well. In this range of $n_s$, presence of the „trion" peak can not be interpreted as formation of the three-particle complexes. Interaction of the exciton with the Fermi sea results in splitting the spectrum of excitations into a low-energy exciton-polaron branch with the energy $\epsilon_T^*$, which is usually identified as the trion, and a high-energy branch with the energy $\epsilon_X^*$, which is identified as the exciton. The calculations [16] were performed to show that splitting between the lines increased linearly from $E_F$ of the equilibrium charge carriers, the trion peak dominated when $E_F \sim E_T$, a width of the trion peak is noticeably smaller than a width of the exciton peak.

It should be noted that the TMD monolayers have a valley degeneracy and strong spin-orbit splitting $\Delta_{so}$. When $E_F < \Delta_{so}$, there are two types of electrons from various valleys, which interact with the excitons. However, if the excitons and the electrons of the Fermi sea belong to the same valley, short-range exchange interaction suppresses correlations. Provided that $E_F \ll E_T$, the exchange interaction does not contribute to formation of trions, except for a large difference of effective masses of the electron and the hole, which is not realized in the TMD. It is assumed that the exciton and a polar electron cloud surrounding it belong to the different valleys. Provided that $E_F \ll E_x$, formability of several Fermi-sea excitations of the electron-hole pairs may be omitted. The photo-excited electron and hole interact both with the excited electron as well as with the hole of the Fermi sea, but interaction with the Fermi hole is significantly less due to smallness of phase space of the hole and it can be omitted. Interaction of the exciton with the Fermi electron, which is a dipole-charge one at large distances, can be approximated by the short-range contact potential (a constant in the momentum representation). The only parameter that characterizes interaction is still the binding energy of the trion, $E_T$, thereby noticeably simplifying an exciton-polaron problem [13–15]. The energy $E_T$ is splitting between the „attracting" and „repelling" polaron lines $\Delta_{XT}$ when $n_s \to 0$, which can be determined experimentally. When $E_F \ll E_T$, a splitting value and redistribution of spectrum weights in absorption are expressed analytically. Specifically,

$$\Delta_{XT} = \epsilon_X^* - \epsilon_T^* = E_T + E_F m_e/\mu_T, \quad (1)$$

$$A_X(\omega, 0) \approx 2\pi Z_T \delta(\omega - \epsilon_T^*) + 2\pi(1 - Z_T)\delta(\omega - \epsilon_X^*) \quad (2)$$

$Z_T = E_F m_e/\mu_T$, $m_e$ — the mass of the electron, $\mu_T$ — the reduced mass of the trion.

The study [18] has calculated the energies of the bound states (the ground state and the excited states) and the scattering states (the continuous spectrum) for three particles in the two-dimensional TMDs. Retardance during scattering of electrons and excitons allowed determining an energy shift at a finite density of the electrons. For these purposes, an effective exciton-electron potential of scattering was proposed, which allowed determining the influence of the electron density on the spectra of optical absorption of TMD in a polaron model. The study [19] has considered a problem of light absorption in the two-dimensional TMDs at intermediate concentrations of the additional charges $E_F \sim E_T$, in terms of exciton polarons. It provides a microscopic derivation of electron-exciton interaction using a variation approach and a perturbation theory. The authors have applied the developed theory for calculating the spectra of absorption and demonstrated that the dependence on the concentration is well explained by a contact-potential model. It is shown in both the studies [18,19] that classical charge-dipole interaction can be used at the large distances.

The polaron theory was generalized in the studies [20,21] for the case of finite temperatures $T$. They used a method of virial expansion of an optical response of the two-dimensional doped semiconductor for the case of high temperatures or low doping, when a temperature wavelength of the electrons is small as compared to the interparticle distance ($T \gg E_F$). It is shown that a traditional trion concept corresponds to a high-temperature and weakly-interacting limit of the Fermi-polaron theory. Using the Fermi-polaron theory at the finite temperature, the authors found a transition from a quantum-degenerate mode with clearly-defined polaron quasiparticles to an incoherent mode at the high temperature or low doping, where the „attracting" polaron quasiparticle with the least energy is destroyed by being absorbed by a wide trion-hole continuum. With an increase of the temperature (or decrease of doping), a profile of radiation of the attracting branch evolves from a symmetrical Lorentz one to an asymmetrical peak with an exponent tail that includes trions and electrons of recoil with a finite momentum.

Determination of the energy of the trion is still a separate problem. The binding energy of the trion was calculated by variation methods [11,22], a method of direct numerical diagonalization for three particles [18,23], a Monte Carlo method [24].

The study [25] has evaluated the energies of the trions and the excitons that are localized on charged donors or acceptors of the TMD monolayers. They were calculated for a logarithmic potential, which fundamentally distinguishes the considered problem from the case of the encapsulated TMD monolayers.

Results of calculations of the binding energy of the trion and other complexes as well as the binding energy of the exciton depend on a substance of the TMD monolayer ($MoS_2$, $MoSe_2$, $WS_2$, $WSe_2$), a monolayer environment (freely suspended, on the substrate, encapsulated by hBN), a type of the used interaction potential (the Coulomb potential or the Rytova–Keldysh potential that takes into account shielding in the monolayer plane [26,27]).

In the present study we have investigated formability of the multi-particle complexes (trions and excitons bound on the impurities) in the encapsulated TMD monolayers and their manifestations in the optical spectra at the low temperatures and the electron concentrations: $T \ll E_F$, $E_T$, $E_x \gg E_T \gg E_F$. The study was aimed at determining a nature of the line that had low energy relative to the exciton line in the spectra of luminescence and reflection, whose interpretation is not singly opinioned at the present. It was tasked to calculate the binding energy and state radii both of the trions and the exciton-impurity complexes within the framework of the same approach.

## 2. Calculations and discussion of results

The calculation was in a two-particle approximation for two kinds of the interaction potentials $V_H$ and $V_S$. At the large distances $r \gg a_{ex}$, dipole-charge interaction was used in both the cases ($r$ — the coordinate in the layer plane, $a_{ex}$ — the exciton radius).

The energy of dipole-charge interaction was determined as the energy of the exciton in the ground state, which is in an electric field of the charge, in the second order of the perturbation theory:

$$V_{ex}(E) = -\frac{1}{2}\alpha_0 E^2, \quad \alpha_0 = 2e^2 \sum_\nu \frac{|x_{0\nu}|^2}{E_0 - E_\nu} \tag{3}$$

$\alpha_0$ — polarizability of the exciton in the ground state. For the point-charge potential $U(r)$ in a medium with permittivity $\epsilon$ at the distance $r$ from the charge $U(r) = -e/(\epsilon r)$, $E = dU/dr = e/(\epsilon r^2)$,

$$V_{ex-e}(r) = -\frac{\alpha_0 e^2}{2\epsilon^2 r^4} \tag{4}$$

It is enough to use this potential in the considered case of the encapsulated TMD layers ($MoSe_2$, $WSe_2$) at the distances $r > a_{ex}$. Generally, the Rytova–Keldysh potential can be used as $U(r)$.

At the small distances, a solid-center model was used for $V_H$: $V_H(r) = V_{ex-e}(r)$, $r > r_{\min}$, $V_H(r_{\min}) \to \infty$ with a cut-off radius $r_{\min} \sim a_x$ [18,28].

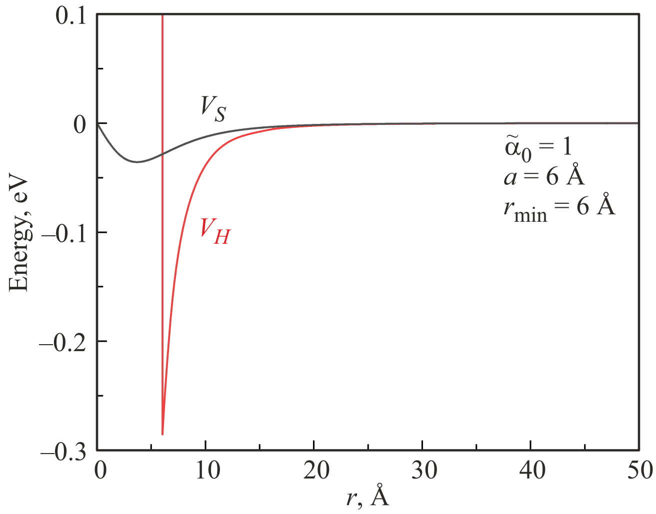


**Figure 1.** Potentials $V_H$ and $V_S$.

At the small distances, interpolation by a smooth potential according to [16,19] was used for $V_S$:

$$V^{eff}_{ex-e} = -\frac{\alpha_0 e^2 r}{2\epsilon^2 (r^2 + a^2)^{5/2}}, \quad a \sim 0.5 a_{ex}. \tag{5}$$

The important parameter of the problem is exciton polarizability $\alpha_0$. This value is known for the two-dimensional exciton with common Coulomb interaction (2DX). The polarizability was calculated both by taking into account only the bound states [28] and by taking into account the continuous-spectrum states [16,19].

$$\alpha_0 = \frac{21}{16}\epsilon a_{ex}^3 \text{ [28]}, \quad \alpha_0 = \frac{8}{5}\epsilon a_{ex}^3 \text{ [16,19]}. \tag{6}$$

If the interaction is different from the Coulomb one, then it is estimated that $\alpha_0 \sim (2–5)\epsilon a_{ex}^3$.

For units of energy and length, we use $E_0 = \mu e^4/(2\hbar^2\varepsilon^2)$, $a_0 = \hbar^2\varepsilon/(\mu e^2)$. For $MoSe_2$ $E_0 = 265$ meV, $a_0 = 6.33$ Å, $(\mu/m_0) = 0.35 m_0$, $m_e/\mu = 2$ ($\mu$ — the reduced mass of the electron and the hole, $m_0$ — the mass of the free electron). For convenience of the calculations, we introduce a dimensionless magnitude of polarizability $\tilde{\alpha}_0$:

$$\alpha_0 = 2\epsilon a_0^3 \tilde{\alpha}_0, \quad \tilde{\alpha}_0 = \alpha_0/(2\epsilon a_0^3) \tag{7}$$

For 2DX $\tilde{\alpha}_0 = 0.08$ ($a_x = a_0/2$). For the exciton in the encapsulated monolayer, it is estimated that $\tilde{\alpha}_0 \sim 2–5$ ($a_{ex} = 0.9$ nm for $MoSe_2$ [5]). For comparison, in atomic units of polarizability $10^{-22}$eV(m/V)$^2$, for 2DX $\alpha_0 = 2.2 \cdot 10^3$, in the encapsulated monolayer $\alpha_0 \sim (60–150) \cdot 10^3$, for the free monolayer (data of the study [18]) $\alpha_0 = 61 \cdot 10^3$.

Figure 1 shows the potentials $V_H$ and $V_S$ for the parameters of $MoSe_2$, the variable parameters $\tilde{\alpha}_0$, $r_{\min}$, $a$ are shown in the figure.

The calculations were carried out for several values of $\tilde{\alpha}_0$ for each of the potentials, and a range of the values

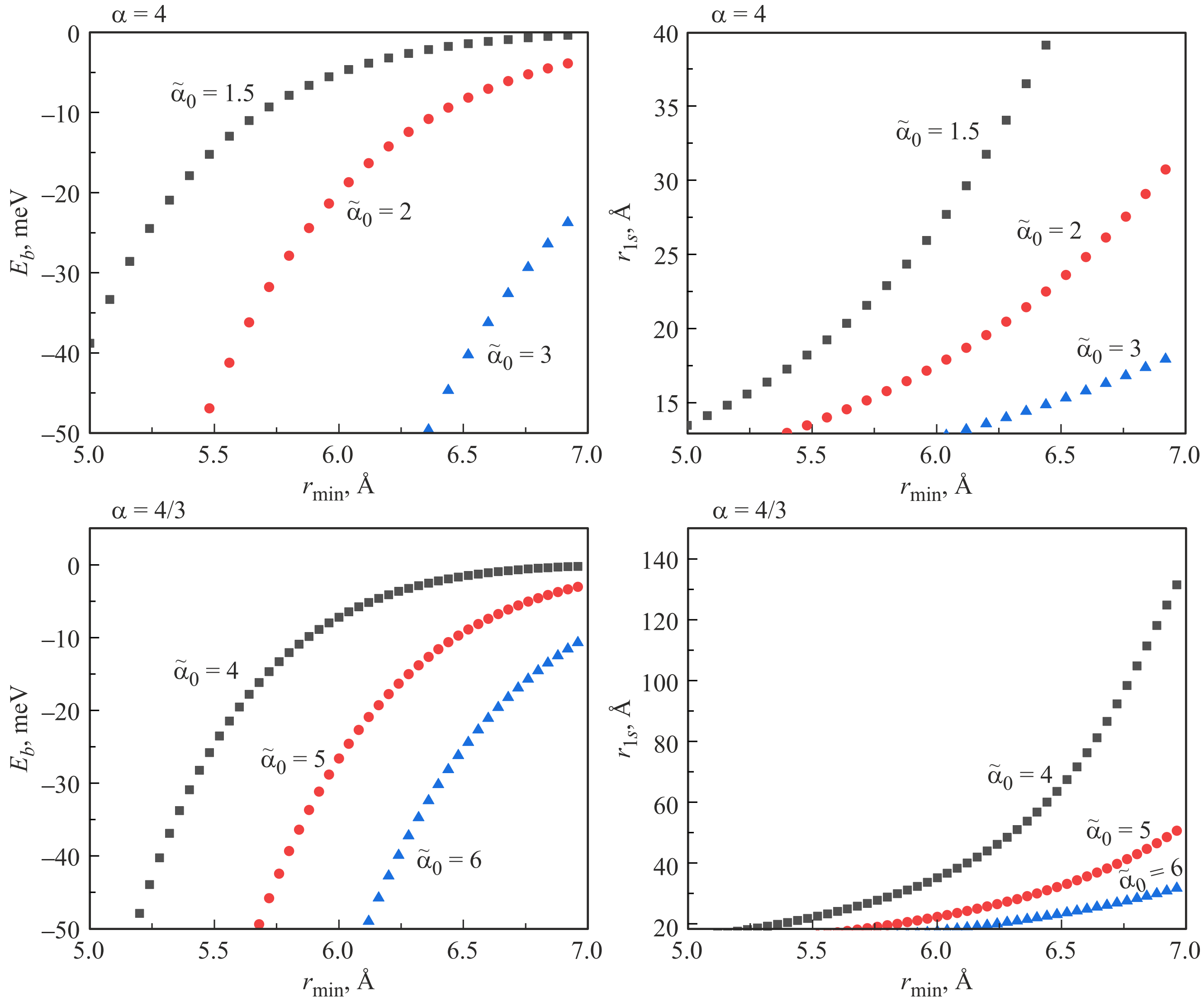


**Figure 2.** Binding energies and the radii of the impurity three-particle complexes ($\alpha = 4$) and the trions ($\alpha = 4/3$) for the potential $V_H$.

was selected so that the obtained binding energies of the complexes were close to the experimental ones (the observed energy gap between the observed lines for the monolayer $MoSe_2 \simeq 26$ meV). Figures 2, 3 shows data of the calculations of the binding energy $E_b$ and the radii of the states $r_{1s}$ of the trions and the impurity complexes in a dependence on the parameters of the used potentials. The reduced mass of the three-particle complex $M = \alpha\mu$, where $\mu$ is the reduced mass of the exciton. For the exciton bound with the charged acceptor the localized exciton, $\alpha = 4$. For the trion, $\alpha = 4/3$.

The calculations for the different potentials are compared to show that qualitative dependences are identical. For the selected value of the energy, the higher polarizability $\tilde{\alpha}_0$, the higher the values of $r_{\min}$ or $a$, and an effective radius of the complex also somewhat increases. For the values of the binding energy $E_b \simeq 26$ meV for the potential $V_H$, the value of polarizability ($\tilde{\alpha}_0 \sim 1.5{-}3$ for $\alpha = 4$ and $\tilde{\alpha}_0 \sim 4{-}6$ for $\alpha = 4/3$) and the radii of the states $r_{1s}$ (15–16 Å and 20–21 Å) are higher than for the potential $V_S$ ($\tilde{\alpha}_0 \sim 0.7{-}1.3$ for $\alpha = 4$ and $\tilde{\alpha}_0 \sim 1{-}2$ for $\alpha = 4/3$, the radii of the states are 11–13 Å, 15–17 Å respectively).

The radii of the states are compared to show arguments in favor of the potential $V_H$. The values of $r_{1s} \sim r_0$ for the potential $V_S$ indicate that it is necessary to apply the Rytova–Keldysh potential for charge-dipole interaction; it is not required for the potential $V_H$, $r_{1s} > r_0$ (the shielding radius $r_0 = 11$ Å [5]). The estimates of polarizability, which are used when comparing the calculations for the impurity complexes and the trions, indicate rather the trions, but an unambiguous conclusion requires a more exact value of $\tilde{\alpha}_0$.

We have also calculated the binding energies $E_b(d)$ and the radii $r_{1s}(d)$ of the impurity three-particle complexes ($\alpha = 4$) in a dependence on the distance of the impurity $d$ from the monolayer for the nearest ($d = 5$ Å) and next ($d = 8.33$ Å) hBN layers [29] for the

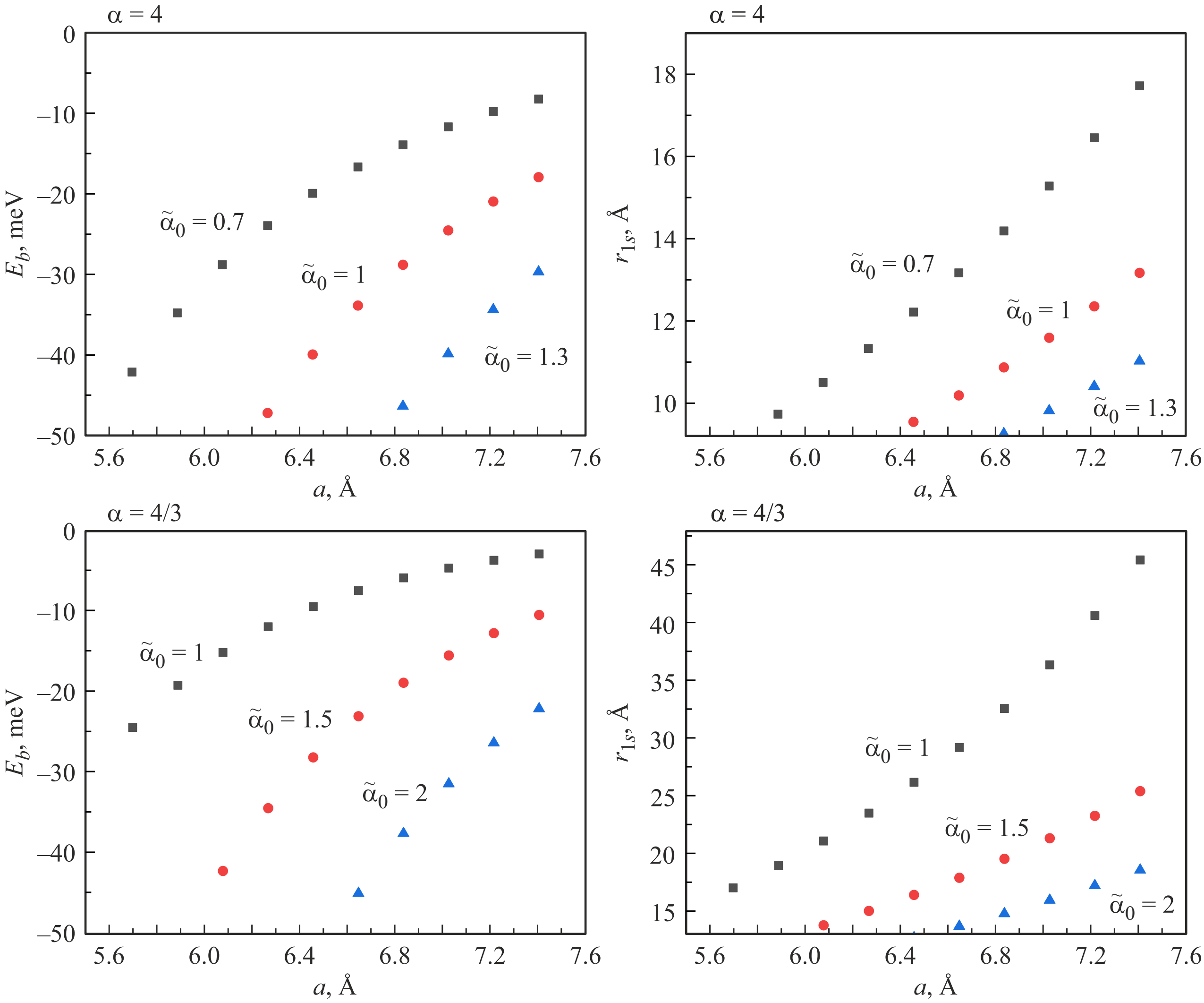


**Figure 3.** Binding energies and the radii of the impurity three-particle complexes ($\alpha = 4$) and the trions ($\alpha = 4/3$) for the potential $V_S$.

potential $\tilde{V}_H$ ($r_{\min} = 5$), $\tilde{\alpha}_0 = 3$.

$$\tilde{V}_H = -\frac{\alpha_0 e^2}{2\epsilon^2 r^4}\left(1 + (d/r)^2\right)^{-3}. \qquad (8)$$

For these parameters within accuracy of the calculations, the impurity complex is formed only for the interface impurity from the nearest hBN layer ($E_b(5\,\text{Å}) = 22\,\text{meV}$, $r_{1s}(5\,\text{Å}) = 17A$, $E_b(8.33\,\text{Å}) = 1.3\,\text{meV}$, $r_{1s}(8.33\,\text{Å}) = 44\,\text{Å}$).

In the hBN-encapsulated monolayers, the equilibrium charge carriers are electrons. Therefore, the prevalent impurities in hBN are of a donor type. The electrons in the monolayer are localized on the interface impurities $D^+$ and the excited excitons could in this case have formed only a four-particle complex ($D^+ + e + X$), whose binding energy is pre-estimated to be small as compared to the complex ($A^- + X$) that is formed by a non-basic acceptor impurity. For the systems with the hole type of doping, the excitons form the complex $D^+ + X$ with the donor impurity. The concentration of the non-basic impurities is small as compared to $n_s$ and their contribution to the studied processes is hardly significant.

As for the spectra of luminescence, there is a dependence not only on the concentration of the equilibrium two-dimensional electrons or holes, but on a method of excitation of the system as well. The excitons can be created using resonance or non-resonant photoexcitation that is stationary or pulsed. In case of stationary non-resonant excitation with a photon energy that noticeably exceeds a band gap, electrons and holes are generated and bound into excitons. The excitons relax in energy and then recombine. For a ratio of intensities of the observed lines of luminescence, in addition to the density of the equilibrium electrons, it is also necessary to take into account a density and an effective temperature of the excitons and the photo-excited electrons and holes. The system is stationary, but is significantly unequilibrated, thereby complicating its description. The present study used this very method of excitation for experimentally studying the spectra of luminescence.

Parameters of approximation of differential reflection coefficients and the data of luminescence of the structures with $MoSe_2$

| Measurement technique | Modeling parameters | Exciton resonances | |
|---|---|---|---|
| | | $A:1s$ | $A:1s^-$ |
| Reflection | $\gamma_0$ (meV)<br>$\gamma$ (meV)<br>$\omega_{res}$ (eV) | 1.5<br>1.2<br>1.639 | 0.05<br>2<br>1.613 |
| Luminescence | FWHM (meV)<br>Peak position (eV) | 2.9<br>1.639 | 3.5<br>1.612 |

Figure 4 shows the experimentally-obtained differential spectrum of reflection and spectrum of luminescence for the structure hBN–ML $MoSe_2$–hBN–$SiO_2$–Si (the experiment and the structure are described in detail by the authors in the study [5]). In the spectrum of reflection, we were able to observe both the ground state of the exciton and energy-lower excitation that is usually associated with the trion (Fermi polaron). The data of approximation of the spectra of reflection and the parameters of the spectra of luminescence are provided in Table. It is clear that the energies of excitations are almost the same for luminescence (PL) and reflection (Refl) (full width at half maximum for the luminescence lines (FWHM) $\sim 3$ meV, Table). An error of a difference of energy positions of the lines $\Delta_{XT} = 26$ meV (Refl), $\Delta_{XT} = 27$ meV (PL) is less than the width of the lines.

For the intensity ratio, the pattern is reversed: in reflection the exciton is manifested much more strongly; in PL, vice versa, the intensity of the exciton lines is much weaker. Values of radiation decay for the excitons and the trions, which are used for approximation of the spectrum of reflection, are $\gamma_{0X} = 1.5$, $\gamma_{0T} = 0.05$, $\gamma_{0X}/\gamma_{0T} = 30$ (see Table). Following the polaron model, one can estimate the concentration of the free electrons in the studied structure (2). $Z_T = \frac{3}{2} E_F/E_T = \gamma_{0T}/\gamma_{0X}$ provides the value of the electron density $n_s = 1.7 \cdot 10^{11}\,\mathrm{cm}^{-2}$, $E_F = 0.58$ meV$=6.5$ K. It should be noted that at 5 K the condition $T < E_F$ is fulfilled, but not $T \ll E_F$ and the value of $n_s$ is rather an estimated one. The study [30] has used a method of quantum well reflection for determining the electron concentration. It was estimated by means of an oscillator force ratio for the trions and the excitons in the magnetic field. The concentrations were previously estimated in the TMD monolayers by a relative shift of the position of the lines of the exciton and the Fermi polaron in luminescence, but not by the intensity ratio in the spectrum of reflection.

In this experiment, the ratio of integral intensities of PL (Figure 4) is $I_T/I_X = 20$. It can be explained as follows. Under the conditions of the experiment (constant non-resonant pumping with the energy that exceeds the band gap), optically active excitons are scarce and they quickly recombine and are not accumulated. The dark excitons are numerous and some of them are bound with all the available electrons and the electrons and holes of the complex recombine. These processes can be more intense. The dark excitons can be both intravalley spin-forbidden ones as well as intervalley ones; it is only required that the joined electron and hole can recombine. Recombination with involvement of the dark excitons was considered in detail in the study [31].

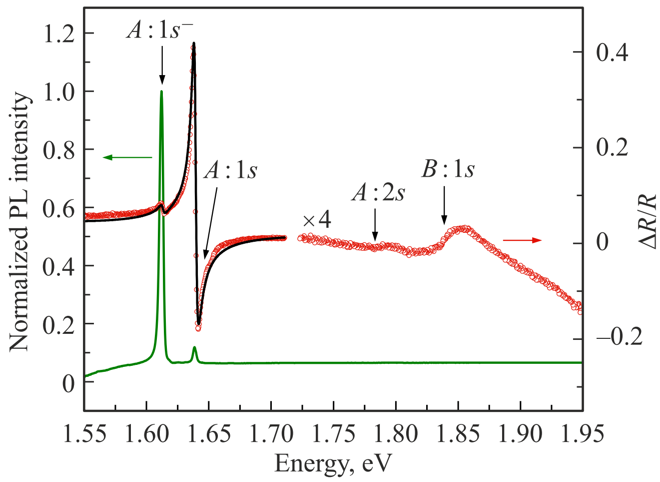


**Figure 4.** Differential spectrum of reflection and the spectrum of luminescence when $T = 5$ K for the structure hBN–ML $MoSe_2$–hBN–$SiO_2$–Si. $A:1s$ – the exciton X, $A:1s^-$ — the charged complex (trion) T.

## 3. Conclusion

The calculated binding energies and radii of states of the three-particle complexes allow existence of both the trions and the excitons that are localized on the charged impurities. The used estimates of polarizability for the energy of the impurity complexes and the trions indicate rather the trions, but the unambiguous conclusion on the nature of the low-energy line in the spectrum and quantitative comparison with the experiment require the exact value of exciton polarizability for specific structures. The potential $V_H$ is more suitable for describing the three-particle complexes. The three-particle complex exists for the exciton that is bound with the interface impurity of the non-basic type, which can be an indirect argument in favor of the trions.

The density of the free electrons in the TMD monolayer has been estimated based on the reflection method.

It would be desirable that the future tasks include consideration of existibility of a trion localized on different-nature inhomogeneities that are large-scale as compared to the radii of the exciton and the trion as well as calculation of the value of polarizability for excitons in the encapsulated monolayers $MoSe_2$ and $WSe_2$.

## Funding

The study was performed under state assignment.

## Conflict of interest

The authors of this paper declare that they have no conflict of interest.

## References

[1] G. Wang, A. Chernikov, M.M. Glazov, T. F. Heinz, X. Marie, T. Aman B. Urbaszek. Rev. Mod. Phys. **90**, 021001 (2018).
[2] M.V. Durnev, M.M. Glazov. UFN **188**, 913 (2018). (in Russian).
[3] M.M. Glazov. J. Chem. Phys. **153**, 034703 (2020).
[4] B. Han, C. Robert, E. Courtade, M. Manca et al. Phys. Rev. **8**, 031073 (2018).
[5] G.M. Golushkov, A.S. Brichkin, V.E. Bisti, A.V. Chernenko. Pis'ma v ZhETF **120**, 279 (2024). (in Russian).
[6] R. Gillen, J. Robertson, J. Maultzsch. Phys. Status Solidi B **251**, 2620 (2014).
[7] A.S. Vokhmintsev, I.A. Weinstein. J. Lum. **230**, 117623 (2021).
[8] Z. Wang, Y.-H. Chiu, K. Honz, K.F. Mak, J. Shan. Nano Lett. **18**, *1*, 137 (2018).
[9] O.V. Volkov, V.E. Zhitomirskii, I.V. Kukushkin, V.E. Bisti, K. fon Klittsing, K. Eberl. Pis'ma v ZhETF **66**, 730 (1997). (in Russian).
[10] O.V. Volkov, I.V. Kukushkin, K. fon Klittsing, K. Eberl. Pis'ma v ZhETF **68**, 223, (1998). (in Russian).
[11] M.A. Semina, R.A. Suris. Phys. Usp. **65**, *2*, 111 (2022).
[12] R. Suris, V. Kochereshko, G. Astakhov, D. Yakovlev, W. Ossau, J. Nurnberger, W. Faschinger, G. Landwehr, T. Wojtowicz, G. Karczewski, J. Kossut. Phys. Stat. Solid. B **227**, 343 (2001).
[13] S. Zoellner, G.M. Bruun, C.J. Pethick. Phys. Rev. A **83**, 021603 (2011).
[14] R. Schmidt, T. Enss, V. Pietila, E. Demler. Phys. Rev. A **85**, 021602 (2012).
[15] V. Ngampruetikorn, J. Levinsen, M.M. Parish. Europhys. Lett. **98**, *3*, 30005 (2012).
[16] D.K. Efimkin, A.H. MacDonald. Phys. Rev. B **95**, 035417 (2017).
[17] M. Sidler, P. Back, O. Cotlet, A. Srivastava, T. Fink, M. Kroner, E. Demler, A. Imamoglu. Nature Phisics **13**, 255 (2017).
[18] C. Fey, P. Schmelcher, A. Imamoglu, R. Schmidt. Phys. Rev. B **101**, 195417 (2020).
[19] D.K. Efimkin, E.K. Laird, J. Levinsen, M.M. Parish, A.H. MacDonald. Phys. Rev. B **103**, 075417 (2021).
[20] B.C. Mulkerin, A. Tiene, F.M. Marchetti, M.M. Parish, J. Levinsen. Phys. Rev. Lett. **131**, 106901 (2023).
[21] A. Tiene, B.C. Mulkerin, J. Levinsen, M.M. Parish, F.M. Marchetti. Phys. Rev. B **108**, 125406 (2023).
[22] E. Courtade, M. Semina, M. Manca, M.M. Glazov, C. Robert, F. Cadiz, G. Wang. Phys. Rev. B **96**, 085302 (2017).
[23] T.C. Berkelbach, M.S. Hybertsen, D.R. Reichman. Phys. Rev. B **88**, 045318 (2013).
[24] M. Szyniszewski, E. Mostaani, N.D. Drummond, V.I. Fal'ko. Phys. Rev. B **95**, 081301(R) (2017).
[25] B. Ganichev, N. Drummond, I. Aleiner, V. Fal'ko. Phys. Rev. Lett. **114**, 107401 (2015).
[26] N.S. Rytova. Vestn. Mosk. un-ta. Ser. 3. Fiz. Astron. **3**, 30 (1967). (in Russian).
[27] L.V. Keldysh. Pis'ma v ZhETF **29**, 716 (1979). (in Russian).
[28] Yu.E. Lozovik, M.V. Nikitkov. ZhETF **111**, 1107 (1997). (in Russian).
[29] V.E. Bisti, A.S. Brichkin, G.M. Golyshkov, A.V. Chernenko. Izvestiya RAN. Seriya fizicheskaya **89**, *2*, 53–57 (2025). (in Russian).
[30] G.V. Astakhov, V.P. Kochereshko, D.R. Yakovlev, W. Ossau, T. Wojtowicz, G. Karczewski, J. Kossut. Phys. Rev. B **65**, 115310 (2002).
[31] Min Yang, Lei Ren, Cedric Robert, Dinh Van Tuan, Laurent Lombez, Bernhard Urbaszek, Xavier Marie, Hanan Dery. Phys. Rev. B **105** 085302 (2022).

*Translated by M.Shevelev*